Ablative Thermal Protection, Thermal Response Characterization, and Integrated Simulation Technique

The Institute of Space and Astronautical Science
Report SP No. 17 March 2003

Thermal Responses of Ablator for Reentry Capsules with Superorbital Velocity

By

Tetsuya YAMADA*, Yoshifumi INATANI*, and Ken'ichi HIRAI†

(1 February 2003)

Abstract: This paper summarizes thermal responses of ablator for reentry capsules with superorbital velocity together with analysis method and the experimental data acquisition in the designing and development process of the MUSES-C reentry capsule. On the prediction of thermo-chemical response of the carbon-phenolic ablator heat shield for the MUSES-C reentry capsule, an ablation analysis code has been developed taking account of the effect of the pyrolysis gas on the surface recession rate. A validation study of the mathematical model for the ablation has been conducted through the comparison between the numerical results and experimental ones which have been carried out in the arcjet facilities of ISAS and NASA/ARC.

1. INTRODUCTION

MUSES-C spacecraft is planned to be launched by M-V rocket in 2003 to make in-situ observations of an asteroid and also to obtain samples of the surface materials (ISAS, 2001). In the final phase of the mission, a small capsule with asteroid sample conducts reentry flight directly from a interplanetary-transfer orbit. The capsule entering with the velocity of 12 km/s is expected to encounter severe aerodynamic heating up to 15 MW/m^2 due to the high reentry speed. The interior of the capsule needs to be thermally protected against the severe aerodynamic heating within a given temperature by the time of landing. The designing and development of the thermal protection system is an important issue for the success of the reentry mission.

It is desired to establish the thermal protection system (TPS) materials necessary and currently available to protect the vehicle in the environments. Based on the preliminary screening tests, carbon phenolic ablator was adopted for the heatshield material of the MUSES-C reentry capsule. A cloth-layered carbon phenolic ablator, which is typical material for solid rocket motor nozzles, is refined and developed especially for the heat shield as 'MC-CFRP'. Because the cloth-layered carbon phenolic has especially large allowable stress in the layer-plane, it

* Institute of Space and Astronautical Science, 3-1-1 Yoshinodai, Sagamihara, Kanagawa, JAPAN.
† IHI Aerospace Company, 900 Fujiki, Tomioka, Gumma, JAPAN.

can function not only thermal protection material but also load-carrying material, which is desirable feature for the heatshield material for small capsules with limited weight budget.

The thermal behavior of the ablator is strongly related to the flight environment such as the flow enthalpy, the impact pressure, and the heat flux. The ground heating facility cannot completely duplicate the flight environment. In order to predict the thermal behavior the ablator in the flight environment based on the ground heating data, it is desired to develop a computational analysis code for the ablation phenomena. Also, for designing the TPS at minimum weight, it is indispensable to develop the code with high accuracy in the prediction of the thermo-chemical behavior of the ablator. Thus, we have conducted a series of arcjet experimental studies to verify the ongoing computational design code (Hirai, et. al., 1998) for the TPS.

The simulation environment of the ground heating test and flight environment is schematically shown in Fig. 1. The heating test environment of ISAS arc heater (Yamada and Inatani, 2002) is limited both in terms of flow enthalpy and in the size of the test pieces. It is desirable to conduct the tests in other facility for correlating and validating the results. Then a series of heating test in 60 MW IHF (Interaction Heating Facility) at NASA ARC was also conducted at the final stage of the qualification process. The major objective is to confirm the ISAS-test-derived results both from view point of the modeling of thermal responses and mechanical durability such as delamination by use of the higher enthalpy flow of 40 MJ/kg and maximum heating of 20 MW/m^2 with model size of 70 mm in diameter.

As shown in Fig. 2, by observing the MC-CFRP test piece (T/P) after the arcjet tests, we can easily find that there exist 4 distinct zones in the T/P, that is to say, lost, charred, decomposed and virgin zone, respectively. Thus, the computational code should be able to predict with high accuracy the positions of these boundaries and the temperature response in the virgin zone.

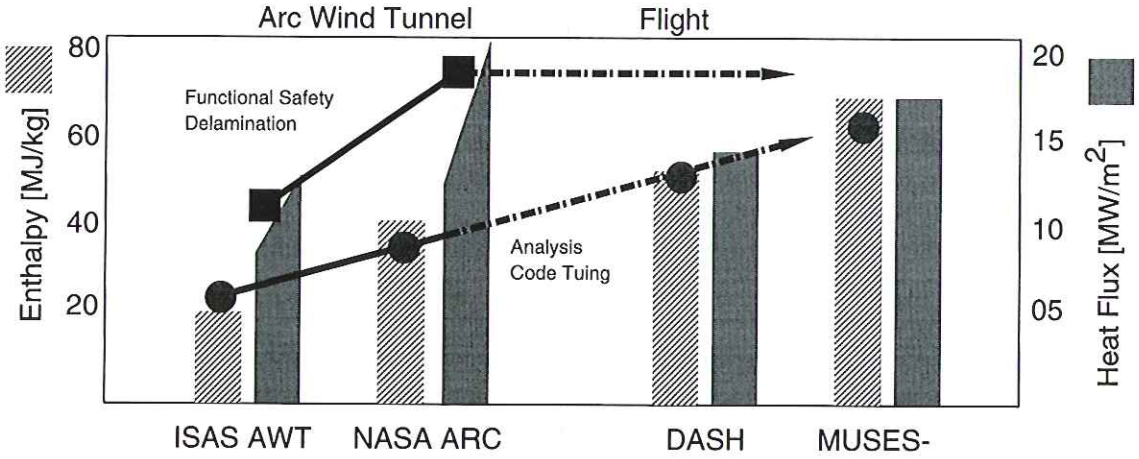

Fig. 1: Simulation Environment of the Ground Heating Test and the Flight Environment.

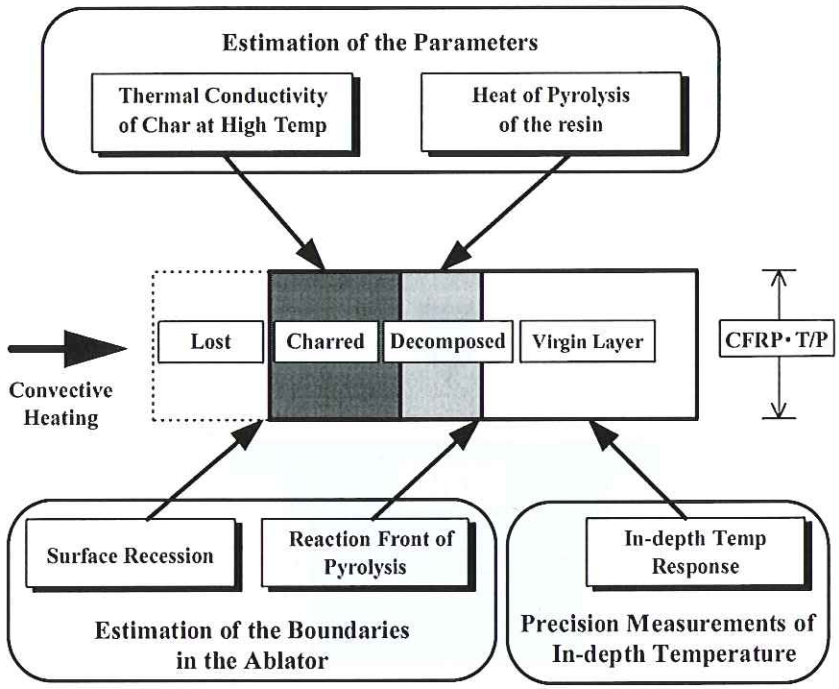

Fig. 2: Schematic of the Carbon Phenolic (MC-CFRP) T/P after the Arc Heating Experiments.

2. THERMAL ANALYSIS OF ABLATION

2.1 Construction of the Mathematical Model

The procedure of constructing the mathematical model for the MC-CFRP ablation phenomena is shown in Fig. 3.

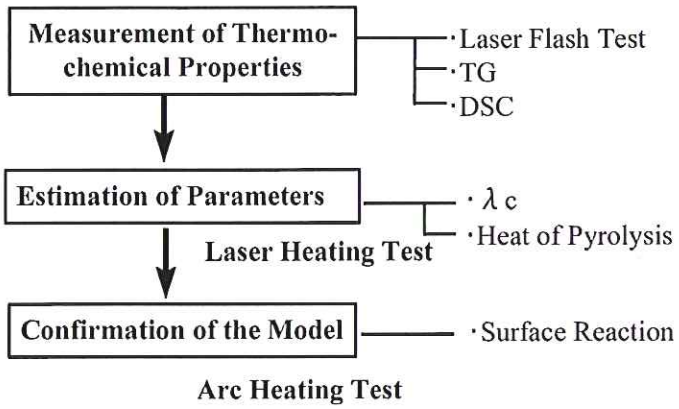

Fig. 3: Procedure of Construction of the Mathematical Model for the MC-CFRP Ablation.

Because of the difficulties in measuring the thermal conductivity of the char at high temper-

ature and heat of pyrolysis, we have made use of laser heating tests under the inert atmosphere, where these parameters are determined by one-dimensional calculations so as to reproduce the surface temperature and char thickness obtained at experiments.

After the thermo-chemical parameters are estimated, arc heating tests are conducted to confirm the mathematical model for the ablation including the surface reaction. The schematic of the MC-CFRP T/P configuration is shown in Fig. 4, where the dual sleeve T/P is adopted to prevent the side wall heating and then to assure the precision measurements of the in-depth temperature (Yamada and Inatani, 2002).

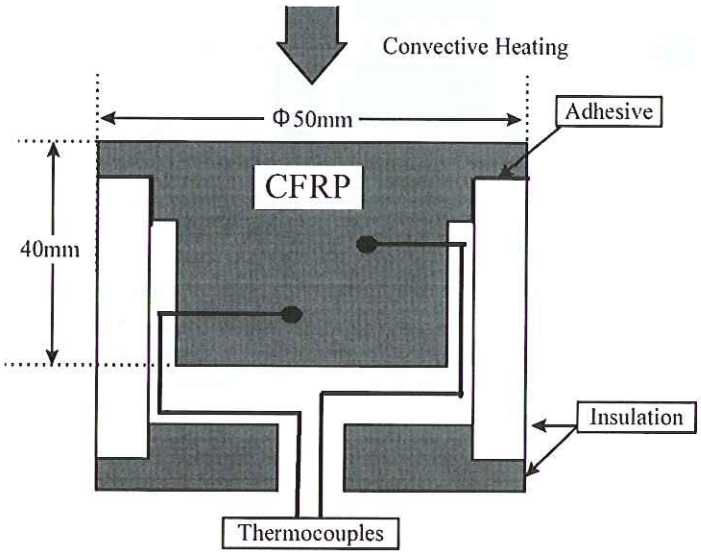

Fig. 4: Schematic of the MC-CFRP T/P Configuration at Arc Heating Experiments.

It is well known that MC-CFRP is thermally expanded when heated. Thus, after each heating test, MC-CFRP T/P is cut in half and the cross section is observed through microscope to estimate the thermal expansion by counting the number of layers. The surface recession due to the surface chemical reaction is determined by subtracting the quantity from the total length change of the T/P.

2.2 Assumptions

The carbon phenolic ablator consists of the resin and carbon cloth. (C-H-O system). As the ablator is heated, the resin begins to decompose at sufficiently elevated temperatures, yielding a pyrolysis gas and a carbon residue (namely, 'char'). As the surface temperature increases, surface reaction between the residue and air becomes activated, and surface recession due to the oxidation reaction or sublimation prevails.

The pyrolysis gas products from the in-depth reaction zone transpires through the heated surface and the venting of the gas products into the boundary layer blocks some of the incident convective heat load (namely, 'blocking effect'). The resin decomposes mainly by endothermic chemical reactions, and the resulting pyrolysis gas products absorb further heat as they percolate to the surface through porous, already charred material.

To simulate the above noted ablation phenomena, one-dimensional energy and mass conservation equations are formulated in a finite difference form implicitly in time. In this paper, the following assumptions are made for simplicity to model the ablation phenomena for the carbon phenolic ablator.
(1)Chemical composition of the char is pure solid carbon.
(2)Chemical reaction between the external flow boundary layer gas and the char occurs only on the surface and this thermo-chemical process causes the surface recession.
(3)Pyrolysis gas product of the carbon phenolic resin is in thermal-equilibrium with the char layer as it percolate through the layer, and also it is inert with respect to the boundary layer gas.
(4)Lewis number of the boundary layer gas is unity so that the mass transfer coefficient equals the heat transfer coefficient.

2.3 Governing Equations

The in-depth governing equations for one-dimensional ablator thermal response are given in the standard expressions (Moyer, et. al., 1968 & Potts, 1995) as follows. In the present scheme, momentum equations are not included.

$$\rho C\frac{\partial T}{\partial \tau} = \frac{\partial}{\partial x}\left(k\frac{\partial T}{\partial x}\right) + \Delta h_G\frac{\partial \rho}{\partial \tau} + \dot{m}_G C_G\frac{\partial T}{\partial x} \tag{1}$$

$$\frac{dC_k}{dt} = -A_k \exp\left(-\frac{\Delta E_k}{RT}\right)(1-C_k)^{n_k} \tag{2}$$

$$\rho = \rho_v - (\rho_v - \rho_c)\sum_{k=1}^{N} f_k C_k \tag{3}$$

$$\frac{\partial \dot{m}_G}{\partial x} = \frac{\partial \rho}{\partial \tau} \tag{4}$$

where Δh_G means heat of pyrolysis per unit mass of gas produced and ρ, C, k, h are the density, specific heat, thermal conductivity and enthalpy of the ablator, respectively, and subscript C, V and G means fully charred state, virgin state, and pyrolysis gas, respectively. Also, τ, x are time, in-depth distance from the surface, and the mass flux of the pyrolysis gas. The momentum equation of the pyrolysis gas should be included for study of the effect of the internal pressure of the pyrolysis gas on the ablator performance such as the delamination, and the attempt is actually under going (Yamada, et. al., 2000). From the standpoint of the accurate estimation of the internal temperature distribution, the present governing equations are enough.

$$\dot{m}_W = \dot{m}_C + \dot{m}_{G,W} \tag{5}$$

$$\dot{q}_{net} = \dot{q}_{conv} - \dot{q}_{rad} - \dot{m}_C(h_W - h_C) \tag{6}$$

where $\dot{q}_{conv}$ means hot wall convective heat rate, which includes the blocking effect.

$$\dot{q}_{conv} = g_h(h_{rec} - h_W) \tag{7}$$

$$\dot{q}_{rad} = \varepsilon\sigma T_W^4 \tag{8}$$

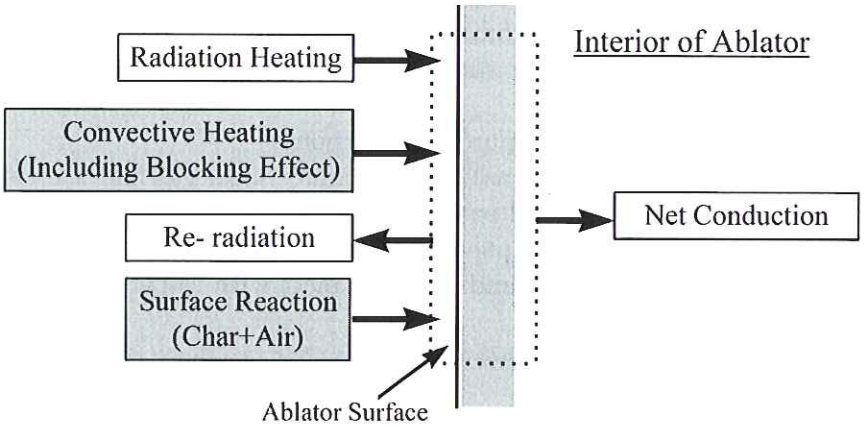

Fig. 5: Schematic of Surface Energy Balance and Semi-infinite Slab of Ablator Material.

where g_h is the heat transfer coefficient, which is the same value as the mass transfer coefficient on the assumption (4). This g_h value is related to the hypothetical cold wall heat transfer value g_{h0} by the following equations.

$$\dot{q}_{CW} = g_{h0} h_{rec} \tag{9}$$

$$g_h = g_{h0} \phi_{blow} \tag{10}$$

where ϕ_{blow} means blocking correction factor. A standard form of this blocking correction factor is shown as follows.

$$\phi_{blow} = \frac{aB_0}{\exp(aB_0) - 1} \tag{11}$$

$$B_0 = \frac{\dot{m}_W}{g_{h0}} = \frac{\dot{m}_C}{g_{h0}} + \frac{\dot{m}_{G,W}}{g_{h0}} = B_{C0} + B_{G0} \tag{12}$$

where the blowing parameter (B_0) can be calculated by using the table ($B_c \sim T_W, P_W$) as will be shown in the next section, and by estimating B_G value timewisely .

2.4 Surface Reaction of the Residue

In the case of carbonaceous ablator, the residue material is assumed pure solid carbon. So, the surface reaction consists in the solid carbon reaction in the air and pyrolysis gas as shown in Fig. 6.

As for the surface recession rate estimation, a bridging formula (Scala's second order transition scheme (Scala, 1965) is applied to smoothly interpolate the two limiting values listed below.

1)surface mass loss rate due to rate-controlled reaction (chemically non-equilibrium)
2)surface mass loss rate due to diffusion rate controlled reaction (chemically equilibrium)

The graphite, air and the pyrolysis gas reaction kinetics expression is used for the former, while, the chemical equilibrium theory is used for the latter. Especially in the higher enthalpy, the effect of the pyrolysis gas on the recession rate turns out not to be negligible. The chemical composition of the MC-CFRP is $C_{2.85}N_{7.54}O$ as shown in Fig. 6. As the result of the

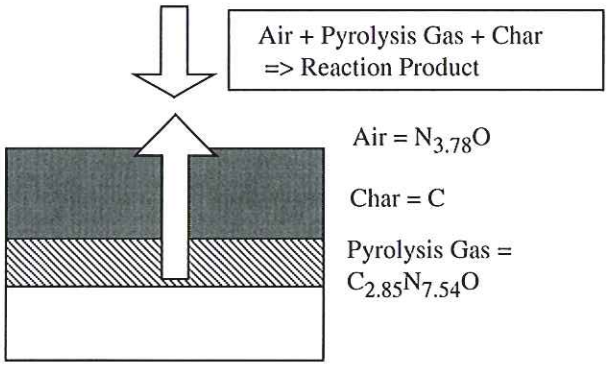

Fig. 6: Concept of the Reaction Model on the Charred Surface.

surface equilibrium thermochemistry, the equilibrium composition, enthalpy of the gas mixture adjacent to the surface, and the non-dimensional mass loss rate is obtained and tabulated for prescribed values of surface pressure and temperature. To compute recession rate, these resultant tables are interpolated.

Figure 7 shows a typical analytical result of nondimensional recession rate at the impact pressure of 1 atm. It is easily recognized from the figure that

1) the char recession rate in the diffusion-controlled region decreases as the nondimensional pyrolysis gas rate decreases (below 3000°C),

2) the char recession rate in the sublimation region increases as the nondimensional pyrolysis gas rate decreases (below 3000°C).

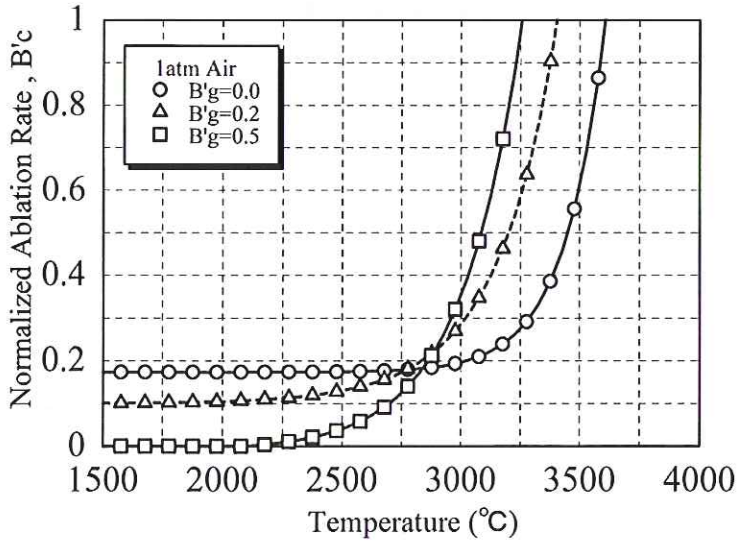

Fig. 7: A Typical Analytical Result of Nondimensional Recession Rate (@1 atm).

For the pure solid carbon, the non-dimensional char mass loss rate (B_C) in air under the assumption (2) is shown in Fig. 10, where the mass loss rate is non-dimensionalized by

the incoming mass flow rate of air. From this figure, we notice that the oxidation reaction prevails in air stream up to the surface temperature around 3000°C, the plateau portion of B_C corresponds to the reaction ($C + O \rightarrow CO$), and sublimation reaction prevails above 3000°C.

2.5 Thermal Decomposition of the Resin

The thermal-decomposition reaction rate of the resin is assumed to follow the Arrhenius kinetic reaction equation and is determined by applying the least square method to reproduce the thermograms of the Thermo-Gravimetric (TG) data. Fig. 8 shows examples of the TG data.

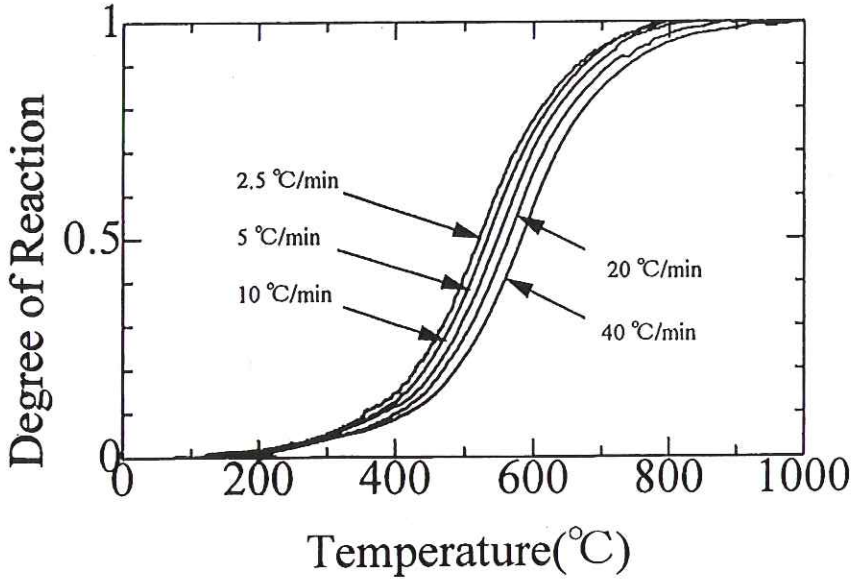

Fig. 8: Examples of Thermogravimetry Curves of MC-CFRP.

The enthalpy and the specific heat of the pyrolysis gas mixture is computed by the equilibrium thermo-chemistry with condensed phase carbon excluded from possible equilibrium products. The chemical formula of the products is assumed to be equal to the elemental composition of the resin minus the percentage of the solid carbon residue.

3. ABLATION ANALYSIS FOR ARCJET MODEL

So far, a series of experimental studies have been carried out in the arcjet facilities of ISAS. The objective is to validate the above noted mathematical model for ablation. This section shows the comparison between the simulation results and experimental results.

3.1 Test Conditions

Due to the test facility limitation, small material samples are tested, which are fabricated in cylinders with 25 or 50mm-diameter. MC-CFRP samples are made of resin-impregnated carbon cloth that is molded in parallel lamina. Test conditions are summarized in Table 1.

Table 1: Arc Heating Test Conditions.

Test Piece Material	MC-CFRP or C/C or Graphite
Convective Cold Wall Heat Flux	$1 - 12$ MW/m^2
Heating Duration	30 sec
Working Gas	Air
Flow Bulk Enthalpy	$10 - 15$ MJ/kg @ISAS
	$-$ 40 MJ/kg @NASA/ARC
Impact Pressure	$60 - 5$ kPa

3.2 Measurements

Measurements of model response are made both during the run and after its completion. Internal temperature measurements are continued for 5 minutes after the heating time. These include:

(1) Surface Recession
(2) Char Thickness
(3) Total Mass Loss
(4) In-depth and Surface Temperature

Some thermocouples are furnished at various locations from the initial top surface. The positions are determined in the preliminary studies so as to record less than 300°C temperature rise during the heat soak period. The heating rate is measured by calorimeter and the surface temperature by one-color pyrometer. After the heating test, MC-CFRP T/P is observed to be slightly thermally expanded. Thus, by eliminating the thermal expansion effect from the measured surface recession, we extract the surface recession due to the surface reaction.

3.3 Thermal Response of the Carbon Phenolic Ablator

Surface Recession

As described in the previous section the nondimensional char recession rate is strongly correlated to the nondimensional pyrolysis gas rate, which is expressed as

$$B'_g \equiv \frac{\dot{m}_g}{\dot{q}_{CW}/h_e} \tag{13}$$

$$\dot{m}_g = \dot{m}_{Total} - \rho_c \cdot \dot{V}_{reces} \tag{14}$$

where ρ_c is the char density and V_{reces} is the recession volume. The time-averaged values of the above equation can be experimentally obtained by measuring the total weight loss m_{Total} and the recession volume under the assumption of constant recession during the heating tests. A series of arc heating tests have been conducted in ISAS, and the data obtained by utilizing NASA ARC have been added into them. Here it needs to be pointed out that the enthalpy level of IHF in ARC ranges up to 40 MJ/kg as was schematically shown in Fig. 1 or Table. 1, then the nondimensional pyrolysis gas rate in ARC is predicted higher than that in ISAS. Figure 9 shows a categorization of B'_g data obtained at ISAS and ARC.

Fig. 10 shows the comparison between the B-prime curve (computed non-dimensionalized recession rate by carbon ablation model, see again Fig. 7) and measured surface recession for

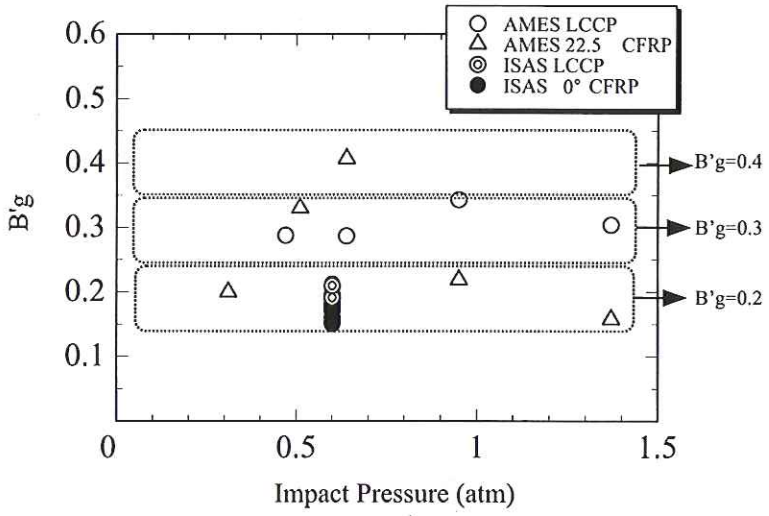

Fig. 9: Categorization of B'_g Data at ISAS/AMES.

several kinds of carbonaceous ablators. Due to the experimental difficulties, the experiments have been carried out under the condition of surface temperature below 3000°C. Although the obtained data show some scatter, the surface recession of the carbonaceous ablators may be approximated by carbon ablation model fairly well.

Figure 11 shows the correlation of the char layer recession rate with parameters of the nondimensional pyrolysis gas blowing rate. The result shows a degree of difference that may be caused by the effects out of the recession modeling. The recession is suggested to be multiplied by 1.6 as an augmentation factor from the standpoint of designing of the thermal protection system. Each reaction rates are calculated under the assumption of chemical equilibrium with respect to the flow impact pressure and enthalpy. The mass flow rate of the ablation products is expressed as non-dimensional gas blowing parameter as a ratio to the mass flow rate of incoming air. They were correlated as a function of the wall temperature on the basis of arc heating test results as shown in Fig 10. The recession data obtained in the heating test are correlated under the assumption that the pyrolysis gas makes chemical reaction with high temperature air in the shock layer.

Char Penetration Depth

Fig. 12 shows the comparison of the measured and computed char penetration depth. From this figure, we find that our numerical code can predict the char penetration depth fairly well.

Blocking Parameters

From the measured value of total mass loss ($\dot{m}_W$), we have estimated the blowing factor (B_0) defined below and then blocking correction factor (ϕ_{blow}).

$$B_0 = \frac{\dot{m}_W}{\dot{q}_{CW}/h_{rec}} \tag{15}$$

Fig. 13 shows these two factors. From this figure, it seems that B_0 ranges $0.15 \sim 0.35$ and $0.8 \sim 0.9$ under the arc heating test conditions.

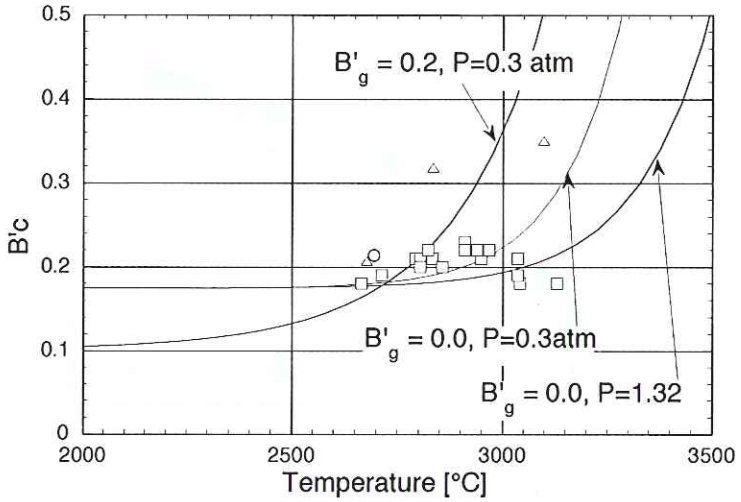

Fig. 10: Bc vs. Wall Temperature Characteristics.

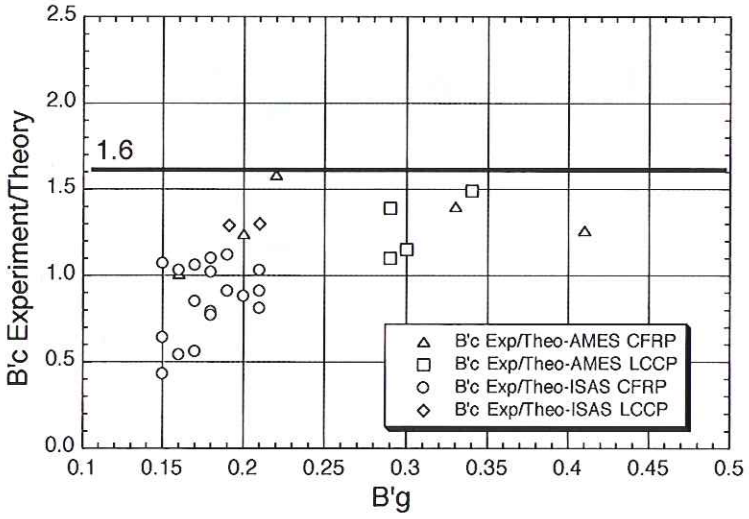

Fig. 11: Comparison of Bc between Experimentally-obtained and Theory.

Reaction Front of Pyrolysis

Fig. 14 shows the measured spatial distribution of peak temperature, where the origin of lateral axis is set equal to the in-depth location of apparent reaction front of pyrolysis, which is obtained from the observation of the post-test T/P. From this figure, the peak temperature at the location is estimated around 300°C, which approximately corresponds to the initiation temperature of pyrolysis from Fig. 8.

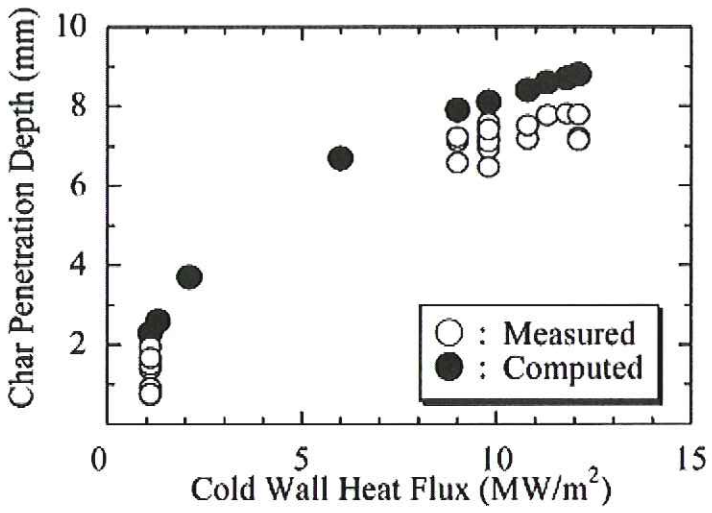

Fig. 12: Comparison of Measured and Computed Char Penetration Depth.

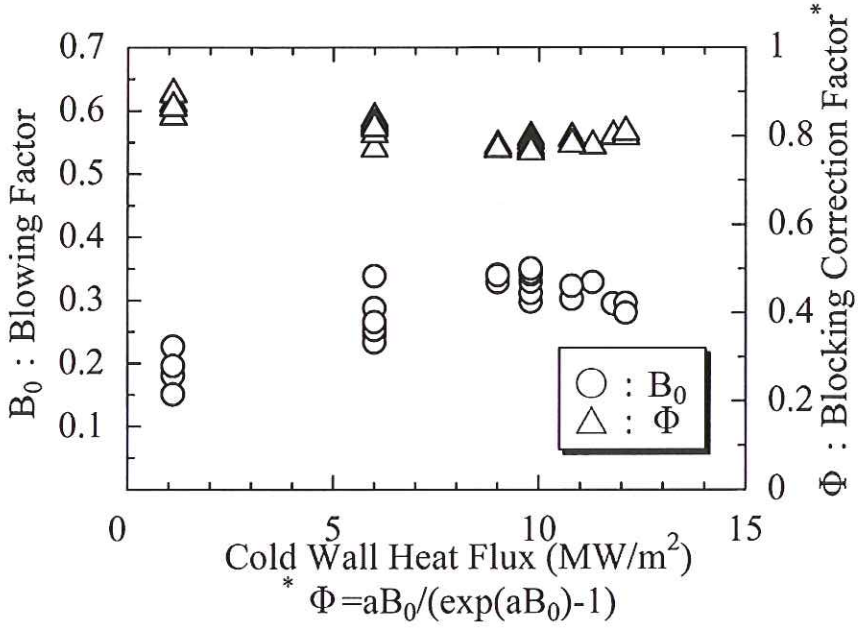

Fig. 13: Estimated Blocking Parameters from Measured Total Mass Loss.

In-depth Temperature Response

Fig. 15 shows the comparison of the measured and computed in-depth temperature response. Due to the experimental difficulties, precision temperature measurements have been carried out only at heating rate of 1 MW/m^2. The shadowed region in the figures represents the uncertainties of T/C locations, which are assumed to be $\pm 0.5mm$. From these figures, we can

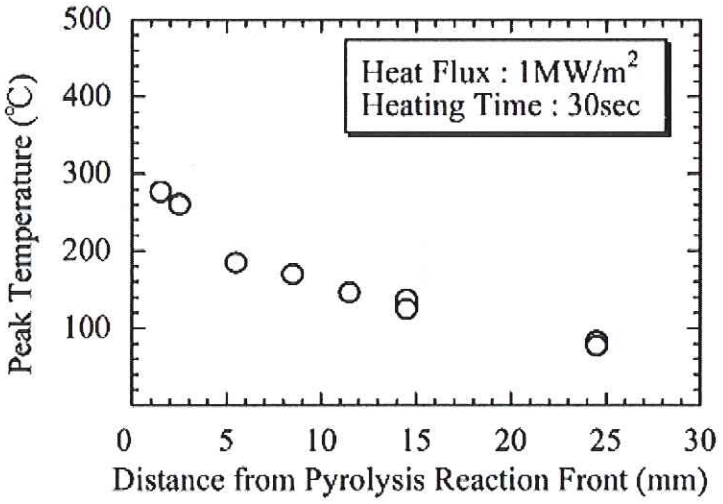

Fig. 14: Measured Spatial Distribution of the Peak Temperature in the T/P.

find that our numerical code can predict the in-depth temperature response fairly well.

Now, precision temperature measurements are planned at heating rate 6 MW/m^2, which corresponds to the maximum heating condition at 50mm-diameter T/P.

4. DISCUSSIONS

So far, the experimental data for the ablation behavior of MC-CFRP have been obtained in the arcjet heating tests at ISAS and NASA/ARC in the heat flux range of 1 to 12 MW/m^2.

As for the carbon phenolic ablator used for the MUSES-C reentry capsule (MC-CFRP) surface recession, the carbon ablation model has been confirmed by the arcjet experiments of the non-dimensionalized recession rate versus surface temperature curve in the temperature range up to 3000°C, which corresponds to the diffusion rate controlled region.

As for the in-depth temperature response of the MC-CFRP, it needs approximately 50mm-diameter T/P to prevent the heating from the side walls of the T/P and to make precision measurements of the in-depth temperature. From above written comparison studies, we have found that the experimental results of the in-depth temperature can be reproduced fairly well by our numerical code under the condition of cold wall heating rate of 1 MW/m^2. The further experimental studies are needed to make the numerical code more reliable.

As for the blocking effect of the MC-CFRP, we have not yet obtained the direct verification of the numerical model. For an indirect approach, the measured surface temperature was compared with the computed radiative equilibrium surface temperature, which is derived from the measured mass loss of the T/P and a tentative mathematical model for the blocking effect from a literature. The experimental results of arcjet tests show that measured surface temperature is approximately equal to the computed radiative equilibrium temperature.

These results are qualitatively equivalent to the results which are obtained in the previous laser heating tests. So far, we have concluded that the numerical model for the blocking is not contradictory to the experimental results of the arcjet heating tests. The blocking effect is supposed to vary with ejected gas species, flow conditions (stagnation point, laminar, or

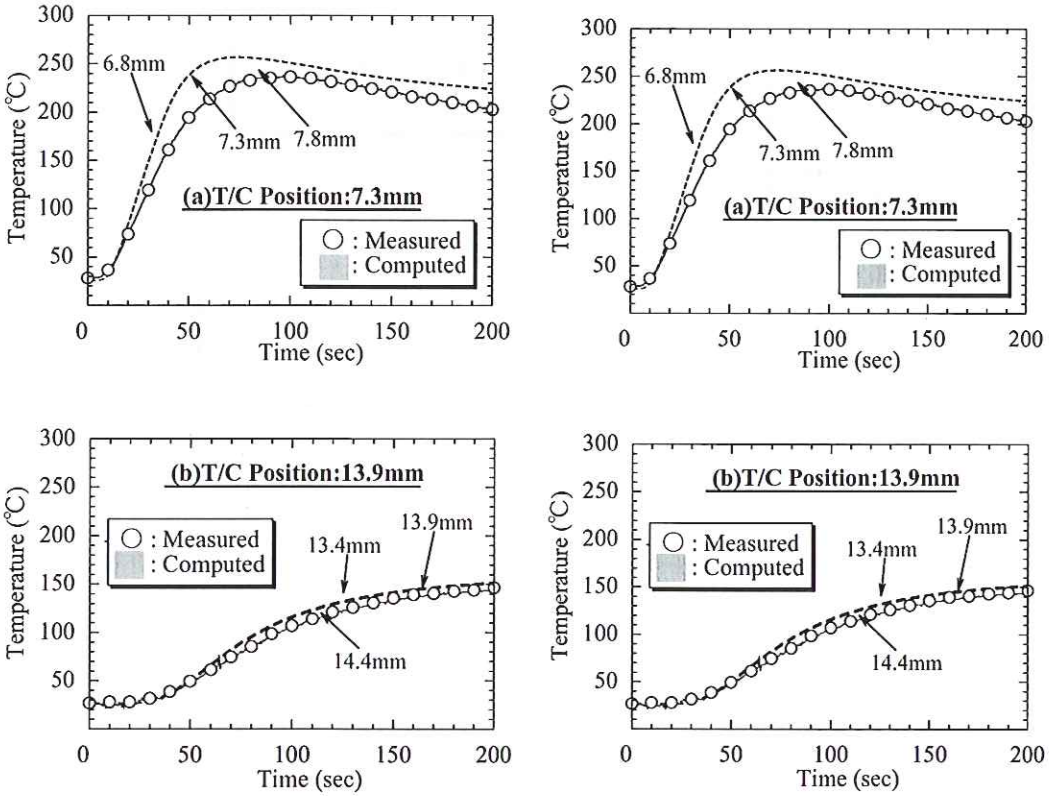

Fig. 15: Comparison of Measured and Computed In-depth Temperature Response (Heat Flux:1 MW/m^2, Duration:30s).

turbulent), and Mach number.

Another important technical issue is the effect of pyrolysis gas on the ply-lifting of the MC-CFRP. In the present study, the pyrolysis gas product of the MC-CFRP resin is assumed to transpire through the charred zone without any hydrodynamic resistance. However, this pyrolysis gas may participate in the surface reaction. Thus, further investigations are needed for this issue.

5. CONCLUSION

So far, the experimental data for the ablation behavior of the carbon phenolic ablator used for the MUSES-C reentry capsule (MC-CFRP) have been obtained in the arcjet heating tests at ISAS and NASA/ARC at the heat flux range of 1 to 12 MW/m^2.

The charring ablation computer code for the prediction of the thermal and recessional response of the carbonaceous ablators has been developed and applied to the numerical simulation studies for arcjet heating tests taking account of the effect of the pyrolysis gas on the total recession rate.

REFERENCES

MUSES-C Mission Plan, MUSES-C Working group, ISAS, March. 2000.

Hirai, K., Shimada, T., Higuchi, S., and Makino, T., "Numerical Simulations of Charring Ablation for the Heat Shields on Surper-orbital Reentry Capsule", Proc. of 21th ISTS, 1998.

Moyer, C.B., and Rindal, R.L., "An Analysis of the Coupled Chemically Reacting Boundary Layer and Charring Ablator, Part 2, Finite Difference Solution for the In-Depth Response of Charring Materials Con-sidering Surface Chemical and Energy Balances", NASA-CR-1061, 1968.

Potts, R. L., "Application of Integral Methods to Ablation Charring Erosion, A Review", J. of Spacecraft and Rockets, Vol. 32, pp. 200–209, 1995.

Scala, S. M., and Gilbert, L. M., "Sublimation of Graphite at Hypersonic Speeds", AIAA Journal, Vol. 3, pp. 1635–1644, 1965.

Yamada, T. and Inatani, Y, "The Effect of Internal Pyrolysis Gas Pressure on the Ablator Performance", Proc. 22nd ISTS, 2000.

Yamada, T. and Inatani, Y, "Arc Heating Facility and Test Technique for Planetary Entry Missions", ISAS Report, 2002.

amada, T., Ishii, N., Inatani, Y., and Honda, M., "Thermal Protection System of the Reentry Capsule with Superorbital Velocity", ISAS Report, 2002.